Confinement-deconfinement crossover in the lattice $\mathbb{C}P^{N-1}$ model

Toshiaki Fujimori,[1,*] Etsuko Itou,[1,2,3,†] Tatsuhiro Misumi,[4,1,5,‡] Muneto Nitta,[1,§] and Norisuke Sakai[1,5,‖]

[1]*Department of Physics, and Research and Education Center for Natural Sciences, Keio University, 4-1-1 Hiyoshi, Yokohama, Kanagawa 223-8521, Japan*
[2]*Department of Mathematics and Physics, Kochi University, Kochi 780-8520, Japan*
[3]*Research Center for Nuclear Physics (RCNP), Osaka University, Osaka 567-0047, Japan*
[4]*Department of Mathematical Science, Akita University, Akita 010-8502, Japan*
[5]*iTHEMS, RIKEN, 2-1 Hirasawa, Wako, Saitama 351-0198, Japan*

(Received 1 August 2019; published 21 November 2019)

The $\mathbb{C}P^{N-1}$ sigma model at finite temperature is studied using lattice Monte Carlo simulations on $S^1_s \times S^1_\tau$ with circumferences L_s and L_τ, respectively, where the ratio of the circumferences is taken to be sufficiently large ($L_s/L_\tau \gg 1$) to approximate the model on $\mathbb{R} \times S^1$. We show that the expectation value of the Polyakov loop undergoes a deconfinement crossover as L_τ is decreased, where the peak of the associated susceptibility gets sharper for larger N. We find that the global $\mathrm{PSU}(N) = \mathrm{SU}(N)/\mathbb{Z}_N$ symmetry remains unbroken in different manners for small and large L_τ, respectively: in the small L_τ region for finite N, the order parameter fluctuates extensively with its expectation value consistent with zero after taking an ensemble average, while in the large L_τ region the order parameter remains small with little fluctuations. We also calculate the thermal entropy and find that the degrees of freedom in the small L_τ regime are consistent with $N-1$ free complex scalar fields, thereby indicating a good agreement with the prediction from the large-N study for small L_τ.

DOI: 10.1103/PhysRevD.100.094506

I. INTRODUCTION

The $\mathbb{C}P^{N-1}$ sigma model [1–4] is known to show up in various aspects of physics. Originally, the $\mathbb{C}P^{N-1}$ models in two dimensions were regarded as toy models of QCD, since they share various common properties such as asymptotic freedom, confinement, generation of a mass gap, and the existence of topological charge. Recently, connections between two dimensional $\mathbb{C}P^{N-1}$ models and four dimensional gauge theories have been established: it appears as the low-energy effective theory on the world volume of a single non-Abelian vortex[1] in the non-Abelian gauge-Higgs model [5–10,10,11] as well as dense QCD [12–15], on a long string of Yang-Mills theory [16], and of an appropriately compactified Yang-Mills theory [17]. In condensed-matter physics, the $\mathbb{C}P^1$ model plays an essential role in the research on the low-energy behavior of antiferromagnetic spin chains and their extensions [18], and it describes a quantum phase transition known as deconfined criticality [19,20], while the $\mathbb{C}P^{N-1}$ model appears as an $\mathrm{SU}(N)$ spin chain [21] and also can be realized in ultracold atomic gases [22,23].

Theoretically, nonperturbative properties of the $\mathbb{C}P^{N-1}$ model have been studied both analytically by the gap equations with the large-N (mean field) approximation [2–4] and by lattice simulations mainly on topological aspects of the model defined on $\mathbb{R}^2$ [24–35]. These analyses are consistent with the Coleman-Mermin-Wagner (CMW) theorem [36,37] forbidding spontaneous breaking of a continuous symmetry in two dimensions, while perturbative analyses are not. Recently, the large-N analyses have been extensively applied to the $\mathbb{C}P^{N-1}$ model at finite temperature, or equivalently the model defined on $\mathbb{R} \times S^1$ with periodic boundary conditions (PBC) [38,39] (see also the earlier works [40,41]). However, these studies do not reach a consensus for physical properties including symmetries at high temperature or at small compactification radius [38,39,42,43] (see also [44–47]), while all studies agree that the CMW theorem is valid at low temperature or

*toshiaki.fujimori018@gmail.com
†itou@yukawa.kyoto-u.ac.jp
‡misumi@phys.akita-u.ac.jp
§nitta@phys-h.keio.ac.jp
‖norisuke.sakai@gmail.com

[1]A single vortex in the $U(N)$ gauge theory with N flavors of Higgs scalar fields in the fundamental representation breaks the $\mathrm{SU}(N)$ flavor symmetry down to $\mathrm{SU}(N-1) \times \mathrm{U}(1)$. Hence the emergent Nambu-Goldstone bosons are described by a $\mathrm{SU}(N)/(\mathrm{SU}(N-1) \times U(1)) = \mathbb{C}P^{N-1}$ nonlinear sigma model at low energies.

at large circumference. We also note that some of the preceding works deal with an analogous case of the model defined on a finite interval [43,48–55]. The questions can be summarized as follows: (i) How the order parameter is defined and how its expectation value depends on the compactification period L_τ. (ii) How the global $\mathrm{PSU}(N) = \mathrm{SU}(N)/\mathbb{Z}_N$ symmetry is realized for finite N. One may naively expect the global symmetry to be broken in the deconfinement phase, where field variables are ordered. It was suggested that the global symmetry is broken in the "deconfinement" phase in the large-N limit [38,39]. On the other hand, the CMW theorem forbids the continuous symmetry breaking at least in finite N. (iii) How the high temperature behavior changes for finite N. In the large-N limit, an explicit high temperature behavior of the free energy was calculated [38].

In this paper, we investigate the $\mathbb{C}P^{N-1}$ model at finite temperature by lattice Monte Carlo simulations to address the above questions. We calculate the Polyakov loop expectation value, its susceptibility and the thermal entropy. Our results can be summarized as follows: (1) We adopt the absolute value of the expectation value of the Polyakov loop as a confinement-deconfinement order parameter. We find that its L_τ dependence exhibits a crossover behavior and the peak of its susceptibility gets sharper with N increases, implying a possible phase transition in the large-N limit [38]. (2) We find that the global $\mathrm{PSU}(N) = \mathrm{SU}(N)/\mathbb{Z}_N$ symmetry remains unbroken in different manners for small and large L_τ, respectively. (3) We calculate the thermal entropy in the small L_τ regime, where the weak-coupling expansion is valid. We show that the result coincides with that for $N-1$ free complex scalar fields, which is in good agreement with the analytical prediction [38] based on the free energy in the large-N limit.

This paper is organized as follows. Section II describes the model in the continuum limit and its lattice setup. The results of the expectation value of the Polyakov loop are shown in Sec. III. In Sec. IV, we focus on the global $\mathrm{PSU}(N) = \mathrm{SU}(N)/\mathbb{Z}_N$ symmetry. In Sec. V, we measure the thermal entropy in the small L_τ regime. Section VI is devoted to a summary and discussions. In the Appendix, we show the analytical calculation of the thermal entropy.

II. MODEL AND LATTICE SETUP

The continuum bare action of the $\mathbb{C}P^{N-1} = \mathrm{SU}(N)/(\mathrm{SU}(N-1)\times\mathrm{U}(1))$ sigma models (without the topological θ-term) is given in terms of an N-component complex scalar field $\phi = (\phi^1, \ldots, \phi^N)$ with the constraint $|\phi|^2 = 1$ as

$$S = \frac{1}{g^2}\int d^2x[\partial_\mu\bar{\phi}\partial_\mu\phi + (\bar{\phi}\partial_\mu\phi)^2]. \tag{1}$$

This can be rewritten in terms of an auxiliary $U(1)$ gauge field A_μ as

$$S = \frac{1}{g^2}\int d^2x D_\mu\bar{\phi}D_\mu\phi, \tag{2}$$

using the covariant derivative $D_\mu\phi = (\partial_\mu + iA_\mu)\phi$. Since the gauge field has no kinetic term, the field equation of A_μ gives $A_\mu \equiv \frac{i}{2}\bar{\phi}\cdot\overleftrightarrow{\partial}_\mu\phi$, and the action (2) reduces to (1) after the elimination of the auxiliary gauge field A_μ. This model has a $\mathrm{PSU}(N) = \mathrm{SU}(N)/\mathbb{Z}_N$ global symmetry, where the $\mathbb{Z}_N$ center is removed since it coincides with a subgroup of U(1) gauge symmetry and is redundant.

On the lattice, the action (2) can be expressed as [24,25,29,30,33]

$$S = N\beta\sum_{n,\mu}(2 - \bar{\phi}_{n+\hat{\mu}}\cdot\phi_n\lambda_{n,\mu} - \bar{\phi}_n\cdot\phi_{n+\hat{\mu}}\bar{\lambda}_{n,\mu}), \tag{3}$$

where ϕ_n is an N-component complex scalar field satisfying $\bar{\phi}_n\cdot\phi_n = 1$ and $\lambda_{n,\mu}$ is a link variable corresponding to the auxiliary U(1) gauge field ($\lambda_{n,\mu} = e^{iA_\mu(n)}$). Here, $n = (n_x, n_\tau)$ labels the sites on the lattice and (n_x, n_τ) run as $n_x = 1, \ldots, N_s$ and $n_\tau = 1, \ldots, N_\tau$, respectively. We also note that $N\beta$ corresponds to the inverse of the bare coupling $\frac{1}{g^2}$. The choice of the lattice action and the over-heat-bath algorithm may be crucial to the purpose of minimizing the computational effort [25].

The spacetime geometry on the lattice is $\mathbb{T}^2 = S^1_s \times S^1_\tau$, where S^1_s and S^1_τ have the circumferences $L_s = N_s a$ and $L_\tau = N_\tau a$, respectively. According to the renormalization group, the following relation between the lattice parameter β and the lattice spacing a holds $\Lambda_{\overline{MS}}a = (2\pi\beta)^{\frac{2}{N}}e^{-2\pi\beta}$, where $\Lambda_{\overline{MS}}$ is defined as a scale at which the renormalized coupling in the $\overline{MS}$ scheme diverges. The lattice Λ scale Λ_{lat} depends on the explicit form of the lattice action. Comparing $\Lambda_{\overline{MS}}$ in Ref. [25] and Λ_{lat} for Eq. (3), we find

$$\Lambda_{\mathrm{lat}}a = \frac{1}{\sqrt{32}}(2\pi\beta)^{\frac{2}{N}}e^{-2\pi\beta-\frac{\pi}{2N}}. \tag{4}$$

It gives a for a given β for each N with Λ_{lat} as a reference scale. This relation is valid for $\beta \gtrsim 1/(\pi N)$, which is comfortably satisfied in this work.

We confirm that the Euclidean energy density $\langle E\rangle = \langle 2 - \bar{\phi}_{n+\hat{\mu}}\cdot\phi_n\lambda_{n,\mu} - \bar{\phi}_n\cdot\phi_{n+\hat{\mu}}\bar{\lambda}_{n,\mu}\rangle$ in our numerical calculations is consistent with the results based on the strong-coupling expansion $\langle E\rangle \approx 2(1-\beta)$ for low β ($\beta \lesssim 0.4$), while it agrees with the result based on weak-coupling expansion $\langle E\rangle \approx 1/(2\beta)$ for high β ($2.0 \lesssim \beta$).

By setting $L_s \gg L_\tau$, we can approximately simulate the model on $\mathbb{R}\times S^1$, where the compactified circumference L_τ is interpreted as an inverse temperature $1/T$. We will mainly use L_τ in this paper, where smaller L_τ (higher β with fixed N_τ) corresponds to higher T. The lattice size in this work is mainly $(N_s, N_\tau) = (200, 8)$.

We also vary N_s between 40 and 200 to look into the finite-volume effects. The thermodynamic limit corresponds to the $N_s \to \infty$ limit. We adopt parameters as $N = 3, 5, 10, 20$ and $0.1 \leq \beta \leq 3.9$.

III. DECONFINEMENT AND POLYAKOV LOOP

The ground state expectation value of a Wilson loop $W(\mathcal{C}) = \mathcal{P}\exp(i \oint_{\mathcal{C}} A)$ is expected to exhibit the exponential area law and perimeter law for a large rectangle with space $\hat{R}$ and Euclidean time $\hat{T}$

$$\langle W(\mathcal{C})\rangle = Ce^{-\sigma\hat{R}\hat{T}-\rho(\hat{R}+\hat{T})}, \tag{5}$$

with the Abelian string tension $\sigma \geq 0$, a constant $\rho \geq 0$ of the perimeter term, and a constant C. The confinement of electrically charged particles is defined by the nonvanishing σ. Actually, in lattice simulations with a large $N_s = N_\tau$, the value of the string tension can be calculated by considering large Wilson loops [25]. If we compactify the temporal direction with a period $L_\tau = N_\tau a$ and impose the PBC, the Wilson loop becomes a correlator of Polyakov loops, $P(x) \equiv \mathcal{P}\exp(i\int_0^{L_\tau} d\tau A_\tau)_x$ at x,

$$\langle W(\mathcal{C})\rangle = \langle P(\hat{R})P^\dagger(0)\rangle. \tag{6}$$

Since the Wilson loop (5) satisfies the clustering property $\langle P(\hat{R})P^\dagger(0)\rangle \to |\langle P\rangle|^2$ in $\hat{R} \to \infty$, the confinement $\sigma \neq 0$ necessitates the vanishing Polyakov loop $\langle P\rangle = 0$. The ground state expectation value of the Polyakov loop $\langle P\rangle$ is a better observable for the confinement-deconfinement transition in the $L_\tau \ll L_s$ system, where taking the large Euclidean time is technically difficult. This picture is based on the analogy to four-dimensional QCD. In the quenched QCD where the $\mathbb{Z}_3$ center of gauge symmetry is exact, $\langle P\rangle$ is an actual order-parameter of the confinement-deconfinement. Even for QCD with fundamental quarks, where the center symmetry is explicitly broken due to the fermion action, $\langle P\rangle$ is often used as an approximate order-parameter of the confinement-deconfinement. The $\mathbb{C}P^{N-1}$ model with PBC has no exact center symmetry, and then the situation here is analogous to four-dimensional QCD with fundamental quarks.

On the lattice, the Polyakov loop is expressed as the product of link variables,

$$P \equiv \frac{1}{N_s}\sum_{n_x}\prod_{n_\tau}\lambda_{n,\tau}. \tag{7}$$

The results for $|\langle P\rangle|$ as a function of β for $N = 3, 5, 10, 20$ are summarized in the left panel of Fig. 1. Here, the lattice parameters are fixed by $(N_s, N_\tau) = (200, 8)$. It clearly shows $|\langle P\rangle| \approx 0$ for low β (large L_τ) and $|\langle P\rangle| \neq 0$ for high β (small L_τ). For intermediate β, the value of $|\langle P\rangle|$ gradually increases especially for small N, as is consistent with a crossover behavior.

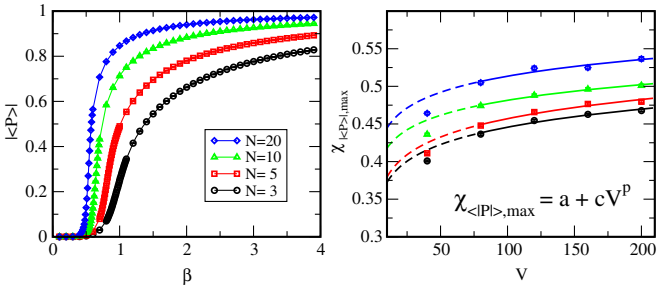

FIG. 1. (Left) The absolute value of expectation value of the Polyakov loop $|\langle P\rangle|$ as a function of β. (Right) The volume dependences of the maximal peak height of the Polyakov loop susceptibility for each N by varying N_s as $N_s = 40, 80, 120, 160, 200$ with $N_\tau = 8$. We fit the four data points with the large volume, $N_s = 80$–200, by a function $\chi_{\langle|P|\rangle,\max} = a + cV^p$.

The corresponding susceptibility of $\langle|P|\rangle$ has a peak, and then we define the characteristic (crossover) length (or the characteristic (crossover) inverse temperature) for each N from the peak position of β. We here consider the susceptibility for $\langle|P|\rangle$ since the β dependences of $|\langle P\rangle|$ and $\langle|P|\rangle$ are almost identical for PBC. We also investigate the heat capacity, $C_v = \langle(E - \langle E\rangle)^2\rangle N_\tau^2$, where E denotes the Euclidean energy density. The heat capacity for each N has the peak at the same value of β as the one for the susceptibility of $\langle|P|\rangle$.

To see the strength of the transition more clearly, we also investigate the volume dependence of the peak value of the Polyakov loop susceptibility, $\chi_{\langle|P|\rangle} = V(\langle|P|^2\rangle - \langle|P|\rangle^2)$, by varying N_s as $N_s = 40, 80, 120, 160, 200$ with $N_\tau = 8$ fixed. We study the scaling with respect to volume, $V = N_s$. We fit the four data points with the large volume, $N_s = 80$–200, by a function $\chi_{\langle|P|\rangle,\max} = a + cV^p$ as shown in the right panel of Fig. 1. The best fit values of the exponent are $p = 0.056(7)$, $0.058(7)$, $0.052(7)$, and $0.043(8)$ for $N = 3, 5, 10$, and 20, respectively. Since it is known that $p = 1$ indicates the first-order transition while $0 < p < 1$ indicates the second-order or crossover transitions [56]. Here, we also look into the $\mathbb{Z}_N$ symmetry of the present model. If we introduce the $\mathbb{Z}_N$ twisted boundary condition for the scalar fields, the $\mathbb{Z}_N$ symmetry, whose order parameter is the expectation value of Polyakov loop, is exact [57–59]. However, in the case of PBC, it is explicitly broken both at small and large L_τ regions. These facts support our argument that the order of the transition is crossover for finite N. Furthermore, all results of the exponent are consistent with each other within $2-\sigma$ statistical error, so that we conclude that there is no clear N-dependence for the strength of the transition in these finite N analyses.

On the other hand, in the large-N limit, we first take the large-N limit with a finite L_τ. To explore the N dependence of the strength of the transition at a finite fixed-volume, the susceptibility of $\langle|P|\rangle$ as a function of a linear scale of $1/L_\tau$ is shown in Fig. 2. Here, the characteristic length (L_c) for

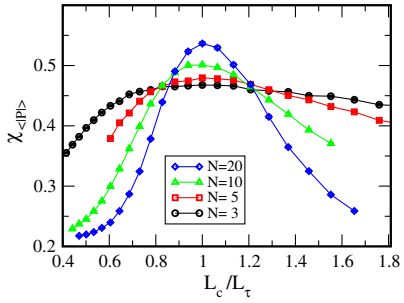

FIG. 2. The susceptibility of the expectation value of absolute value of Polyakov loop $\langle|P|\rangle$ as a function of L_c/L_τ for $N = 3, 5, 10, 20$ with $(N_s, N_\tau) = (200, 8)$.

each N is defined from the peak position of β with fixed $(N_s, N_\tau) = (200, 8)$ simulations, and β is translated into the length $L_\tau = N_\tau a$ via Eq. (4). The N dependence of the susceptibility indicates that the peak is quite broad for small N but it gets sharper as N increases. This result suggests that the order of transition is crossover for finite N while it is possibly transformed into a phase transition in the large-N limit as conjectured in Ref. [38].

IV. GLOBAL PSU(N) SYMMETRY

It was claimed in Ref. [38] that the deconfinement phase transition is associated with the PSU(N) symmetry breaking in the large-N analysis while, at finite N, the PSU(N) global symmetry is never broken in two-dimensions even at finite temperature because of the CMW theorem. Now, we found the confinement and deconfinement phases even for finite N, then the questions arise: whether the PSU(N) symmetry exists in the deconfinement phase and, if it exists, how the symmetry is realized in the phase.

To look into this property, we calculate the following $N \times N$ matrix quantity,

$$P^{ij} \equiv \sum_n \bar{\phi}_n^i \phi_n^j - \frac{1}{N}\delta^{ij}, \quad i, j = 1, \ldots, N \tag{8}$$

whose expectation value serves as an order parameter of the PSU(N) symmetry in the $\mathbb{C}P^{N-1}$ model. The distributions of the diagonal components P^{ii} $(i = 1, 2, 3)$ with $N = 3$ for the confinement phase $(\beta = 0.1)$ and the deconfinement phase $(\beta = 3.9)$ are presented in Fig. 3. The horizontal axis stands for the label number of configurations, where we pick up one configuration per 5000 sweeps. In the confinement phase, the values of $|P^{ii}|$ are relatively small for all the configurations and lead to $\langle P^{ii}\rangle \approx 0$ as $\langle P^{11}\rangle = -2.80(5808) \times 10^{-5}$, $\langle P^{22}\rangle = 3.31(553) \times 10^{-4}$, $\langle P^{33}\rangle = -3.03(589) \times 10^{-4}$. On the other hand, in the deconfinement phase, the values of P^{ii} for some of configurations are far from zero and are distributed broadly. The expectation values for this case is, however, still consistent with zero, where $\langle P^{11}\rangle = -8.22 \times 10^{-4}$, $\langle P^{22}\rangle = 1.48 \times 10^{-6}$, $\langle P^{33}\rangle = 8.21 \times 10^{-4}$ with $O(10^{-2})$

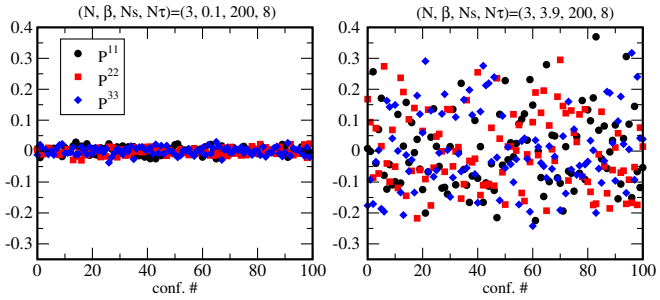

FIG. 3. P^{ii} $(i = 1, 2, 3)$ with $N = 3$ for $\beta = 0.1$ (confinement) (left) and $\beta = 3.9$ (deconfinement) (right) are shown. The horizontal axis stands for the label number of configurations and we pick up one per 5000 sweeps.

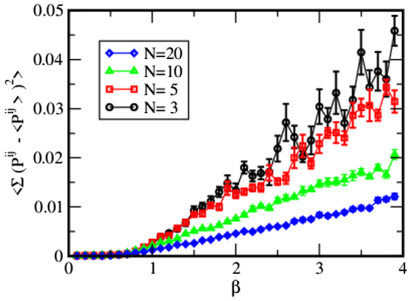

FIG. 4. The variance of P^{ij} for $N = 3$, 5, 10, and 20 as a function of β are shown.

statistical errors. We can conclude that PSU(N) symmetry is realized after taking an ensemble average in the deconfinement phase where the field variables on each configuration are ordered. It is in contrast to the confinement phase, in which it is realized for each configuration.

We carry out a similar analysis also for $N = 5$, 10, 20. The variance of the P^{ij}, which is given by the ensemble average of $\sum_{ij}(P^{ij} - \langle P^{ij}\rangle)^2$, fluctuates more in the deconfinement phase as shown in Fig. 4. It is still an open question whether or not this global symmetry is broken in the large-N limit.

V. THERMAL ENTROPY DENSITY

Now, we numerically find that all N components of ϕ^i are equivalent even in the deconfinement phase, but the actual number of degrees of freedom (d.o.f.) must be $N - 1$ due to one constraint, $|\phi|^2 = 1$. To show it manifestly, let us study the thermal entropy density (s), which counts the d.o.f. of the system, in the deconfinement phase.

In finite temperature (quenched) QCD, the thermal entropy has been calculated in two independent ways; from the energy-momentum tensor (EMT) and the free energy. It has been confirmed that these approaches give consistent results [60]. We first focus on the EMT before considering the free energy. We define the following quantities as a lattice EMT:

$$T_{\tau\tau} = 2N\beta(2 - \bar{\phi}_{n+\tau}\cdot\phi_n\lambda_{n,\tau} - \bar{\phi}_n\cdot\phi_{n+\tau}\bar{\lambda}_{n,\tau}) - (\text{trace part}). \tag{9}$$

T_{xx} can be defined as well. The vacuum expectation value of the trace part is subtracted, in a manner parallel to the lattice EMT for the $O(N)$ sigma model [61,62].

Although the renormalized coupling is required for calculation of the renormalized EMT in principle, we can use the bare coupling constant since it is a good approximation in the weak coupling regime (see e.g., Eq. (6.12) in Ref. [61]). The thermal entropy density is given by $T_{xx} - T_{\tau\tau} = sT$ with $T \equiv 1/L_\tau$ in the thermodynamic limit, where the divergent part of the EMT is cancelled between the two terms.

The results of the thermal entropy density for single scalar field for $N = 3, 5, 10, 20$ as a function of β are shown in Fig. 5. The thermal entropy density becomes nonzero around a certain β corresponding to L_c and monotonically grows in the deconfinement phase. For high-β regions, the β dependence gets gentler for each N, where we fit them by a function $g(\beta) = a + b/\beta$ between $3.0 \le \beta \le 3.9$. The best fit values of a are $a_{N=3} = 1.418(27)$, $a_{N=5} = 1.681(26)$, $a_{N=10} = 1.889(29)$, $a_{N=20} = 2.024(30)$. We then find that the values in the $\beta \to \infty$ limit are 1.2σ consistent with $2\pi(N-1)/(3N)$.

On the other hand, the free energy density for a free massive complex scalar field at finite temperature ($T = 1/L_\tau$) is given by

$$f = \frac{1}{L_\tau L_s}\sum_{n=-\infty}^{\infty} \log 4\sinh^2\frac{L_\tau\omega_n}{2} - f_0 \tag{10}$$

from the analytical calculation (see Appendix). Here, $\omega_n^2 = (\frac{2\pi n}{L_s})^2 + m^2$ and f_0 denotes the counterterm which cancels the UV divergence. Then, the thermal entropy density in the massless and thermodynamic limit ($L_s \to \infty$) is given by $s/T = -\frac{1}{T}\frac{\partial f}{\partial T} = \frac{2\pi}{3}$ for a one-component complex scalar field. Our numerical results indicate that the actual d.o.f. of the $\mathbb{C}P^{N-1}$ model is $(N-1)$ massless free complex scalar fields in the deconfinement phase. Furthermore, the large-N limit of our results is consistent with the prediction calculated from the free energy for the large-N limit in the small L_τ regime, $f = -\frac{N\pi}{3L_\tau^2}$ [38,63–65] using similar calculations.

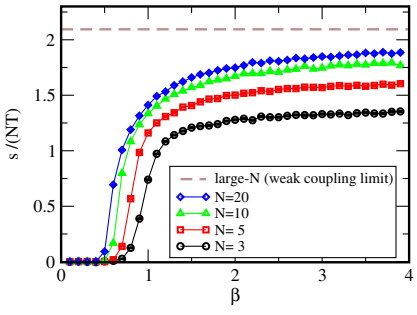

FIG. 5. Thermal entropy density for single ϕ ($s/(NT) = N_\tau^2\langle T_{xx} - T_{\tau\tau}\rangle/N$) for $N = 3, 5, 10, 20$. The dotted line denotes the large-N results in the small L_τ regime, $2\pi/3$.

VI. SUMMARY AND DISCUSSION

In this paper, we have reported the results on nonperturbative aspects of the $\mathbb{C}P^{N-1}$ model on $S^1(\text{large})\times S^1(\text{small})$: We have found a confinement-deconfinement crossover by calculating the L_τ dependence of the expectation value of the Polyakov-loop, where the peaks of its susceptibility get shaper as N increases. We have clearly shown that the global $\mathrm{PSU}(N) = \mathrm{SU}(N)/\mathbb{Z}_N$ symmetry remains unbroken in different manners for small and large L_τ, although the CMW theorem is satisfied in both regions. We have obtained the thermal entropy in the small L_τ regime, which was shown to agree with the prediction from the large-N study.

Our results give a new insight into the phase diagram of the $\mathbb{C}P^{N-1}$ model. Furthermore, since some of the conjectures we have discussed originate in four-dimensional gauge theories, our results also would give possible implications to four-dimensional gauge theories.

As a future avenue, this work can be extended to the model with different geometries and/or boundary conditions, such as the model on $\mathbb{R}\times S^1$ with $\mathbb{Z}_N$ twisted boundary conditions, where the $\mathbb{Z}_N$ symmetry is exact [57–59], and the model on a finite interval for which the Casimir effect is extensively argued [43,48–55]. For the former, whether it undergoes a first-order phase transition or has adiabatic continuity of the vacuum structure [66], and whether fractional instantons have physical consequences [10,34,67–76] in the model, are questions attracting a great deal of attention in terms of the resurgence theory of the models [57,58,75–82].

ACKNOWLEDGMENTS

This work is supported by the Ministry of Education, Culture, Sports, Science, and Technology(MEXT)-Supported Program for the Strategic Research Foundation at Private Universities "Topological Science" (Grant No. S1511006) and by the Japan Society for the Promotion of Science (JSPS) Grant-in-Aid for Scientific Research (KAKENHI) Grant No. (18H01217). This work is also supported in part by JSPS KAKENHI Grant Numbers 19K03875 (E. I.), 18K03627 (T. F.), 19K03817 (T. M.), and 16H03984 (M. N.). The work of M. N. is also supported in part by a Grant-in-Aid for Scientific Research on Innovative Areas "Topological Materials Science" (KAKENHI Grant No. 15H05855) from MEXT of Japan. Numerical simulations were performed on SX-ACE at the Cybermedia Center, Osaka University and TSC at Hiyoshi Department of Physics, Keio University.

APPENDIX: THERMAL ENTROPY OF A FREE MASSIVE SCALAR FIELD

In this Appendix, we calculate the thermal entropy of a free massive scalar field

$$S = \int d^2x(|\partial_\mu \phi|^2 + m^2|\phi|^2). \tag{A1}$$

On a torus with periods (L_s, L_τ), this model can be regarded as a collection of infinitely many 2D harmonic oscillators with frequencies $\omega_n^2 = (\frac{2\pi n}{L_s})^2 + m^2$ at temperature $T = 1/L_\tau$, so that the partition function is given by

$$Z = \prod_{n=-\infty}^{\infty} \frac{1}{4\sinh^2 \frac{L_\tau \omega_n}{2}}. \tag{A2}$$

The free energy density f can be obtained from $Z = e^{-L_\tau L_s f}$ as

$$f = \frac{1}{L_\tau L_s} \sum_{n=-\infty}^{\infty} \log 4\sinh^2 \frac{L_\tau \omega_n}{2} - f_0, \tag{A3}$$

where the last term denotes the counterterm which cancels the UV divergence. In the infinite volume limit $L_s \to \infty$, the summation over the Kaluza-Klein momentum is replaced by the momentum integration

$$f = \frac{1}{L_\tau} \int \frac{dk}{2\pi} \log 4\sinh^2 \frac{L_\tau \sqrt{k^2 + m^2}}{2} - f_0. \tag{A4}$$

The energy density can be calculated from this free energy as

$$\begin{aligned} \epsilon &= \frac{\partial}{\partial L_\tau}(L_\tau f) \\ &= \int \frac{dk}{2\pi} \sqrt{k^2 + m^2} \coth \frac{L_\tau}{2} \sqrt{k^2 + m^2} - f_0. \end{aligned} \tag{A5}$$

From these expressions, we find that the high temperature (small L_τ) behavior of the thermal entropy density in the infinite volume limit takes the form

$$s = L_\tau(\epsilon - f) = \frac{1}{L_\tau}\left[\frac{2\pi}{3} + \mathcal{O}(L_\tau m)\right]. \tag{A6}$$

It is notable that s is independent of the choice of the counterterm. Since the pressure in the infinite volume limit can be written as

$$P = -\frac{\partial}{\partial L_s}(L_s f) = -f, \tag{A7}$$

the thermal entropy density can also be written as $s = L_\tau(\epsilon + P)$.

[1] H. Eichenherr, Nucl. Phys. **B146**, 215 (1978); **B155**, 544 (1979).
[2] E. Witten, Nucl. Phys. **B149**, 285 (1979).
[3] A. D'Adda, M. Luscher, and P. Di Vecchia, Nucl. Phys. **B146**, 63 (1978).
[4] A. D'Adda, P. Di Vecchia, and M. Luscher, Nucl. Phys. **B152**, 125 (1979).
[5] A. Hanany and D. Tong, J. High Energy Phys. 07 (2003) 037.
[6] R. Auzzi, S. Bolognesi, J. Evslin, K. Konishi, and A. Yung, Nucl. Phys. **B673**, 187 (2003).
[7] M. Eto, Y. Isozumi, M. Nitta, K. Ohashi, and N. Sakai, Phys. Rev. Lett. **96**, 161601 (2006).
[8] M. Eto, K. Konishi, G. Marmorini, M. Nitta, K. Ohashi, W. Vinci, and N. Yokoi, Phys. Rev. D **74**, 065021 (2006).
[9] D. Tong, arXiv:hep-th/0509216.
[10] M. Eto, Y. Isozumi, M. Nitta, K. Ohashi, and N. Sakai, J. Phys. A **39**, R315 (2006).
[11] M. Shifman and A. Yung, Rev. Mod. Phys. **79**, 1139 (2007); *Supersymmetric Solitons* (Cambridge University Press, Cambridge, England, 2009).
[12] E. Nakano, M. Nitta, and T. Matsuura, Phys. Rev. D **78**, 045002 (2008).
[13] M. Eto, E. Nakano, and M. Nitta, Phys. Rev. D **80**, 125011 (2009).
[14] M. Eto, M. Nitta, and N. Yamamoto, Phys. Rev. Lett. **104**, 161601 (2010).
[15] M. Eto, Y. Hirono, M. Nitta, and S. Yasui, Prog. Theor. Exp. Phys. **2014**, 012D01 (2014).
[16] O. Aharony and Z. Komargodski, J. High Energy Phys. 05 (2013) 118.
[17] M. Yamazaki and K. Yonekura, J. High Energy Phys. 07 (2017) 088.
[18] F. D. M. Haldane, Phys. Lett. **93A**, 464 (1983).
[19] T. Senthil, A. Vishwanath, L. Balents, S. Sachdev, and M. P. A. Fisher, Science **303**, 1490 (2004).
[20] F. S. Nogueira and A. Sudbø, Europhys. Lett. **104**, 56004 (2013).
[21] B. B. Beard, M. Pepe, S. Riederer, and U. J. Wiese, Phys. Rev. Lett. **94**, 010603 (2005).
[22] C. Laflamme, W. Evans, M. Dalmonte, U. Gerber, H. Mejia-Diaz, W. Bietenholz, U.-J. Wiese, and P. Zoller, Ann. Phys. (Amsterdam) **370**, 117 (2016).
[23] K. Kataoka, S. Hattori, and I. Ichinose, Phys. Rev. B **83**, 174449 (2011).
[24] B. Berg and M. Luscher, Nucl. Phys. **B190**, 412 (1981).
[25] M. Campostrini, P. Rossi, and E. Vicari, Phys. Rev. D **46**, 2647 (1992).
[26] M. Campostrini, P. Rossi, and E. Vicari, Phys. Rev. D **46**, 4643 (1992).

[27] F. Farchioni and A. Papa, Phys. Lett. B **306**, 108 (1993).
[28] R. Burkhalter, Phys. Rev. D **54**, 4121 (1996).
[29] B. Alles, L. Cosmai, M. D'Elia, and A. Papa, Phys. Rev. D **62**, 094507 (2000).
[30] J. Flynn, A. Juttner, A. Lawson, and F. Sanfilippo, arXiv: 1504.06292.
[31] F. Bruckmann, C. Gattringer, T. Kloiber, and T. Sulejmanpasic, Phys. Lett. B **749**, 495 (2015); **751**, 595(E) (2015).
[32] F. Bruckmann, C. Gattringer, T. Kloiber, and T. Sulejmanpasic, Phys. Rev. D **94**, 114503 (2016).
[33] Y. Abe, K. Fukushima, Y. Hidaka, H. Matsueda, K. Murase, and S. Sasaki, arXiv:1805.11058.
[34] F. Bruckmann and S. Lochner, Phys. Rev. D **98**, 065005 (2018).
[35] C. Bonanno, C. Bonati, and M. D'Elia, J. High Energy Phys. 01 (2019) 003.
[36] S. R. Coleman, Commun. Math. Phys. **31**, 259 (1973).
[37] N. D. Mermin and H. Wagner, Phys. Rev. Lett. **17**, 1133 (1966).
[38] S. Monin, M. Shifman, and A. Yung, Phys. Rev. D **92**, 025011 (2015).
[39] S. Monin, M. Shifman, and A. Yung, Phys. Rev. D **93**, 125020 (2016).
[40] S. I. Hong and J. K. Kim, Phys. Rev. D **50**, 2942 (1994).
[41] S. I. Hong and J. K. Kim, J. Phys. A **27**, 1557 (1994).
[42] S. Bolognesi, S. B. Gudnason, K. Konishi, and K. Ohashi, arXiv:1905.10555.
[43] A. Flachi, G. Fucci, M. Nitta, S. Takada, and R. Yoshii, Phys. Rev. D **100**, 085006 (2019).
[44] M. Nitta and R. Yoshii, J. High Energy Phys. 12 (2017) 145.
[45] M. Nitta and R. Yoshii, J. High Energy Phys. 09 (2018) 092.
[46] M. Nitta and R. Yoshii, J. High Energy Phys. 08 (2018) 007.
[47] R. Yoshii and M. Nitta, Symmetry **11**, 636 (2019).
[48] A. Milekhin, Phys. Rev. D **86**, 105002 (2012).
[49] S. Bolognesi, K. Konishi, and K. Ohashi, J. High Energy Phys. 10 (2016) 073.
[50] A. Milekhin, Phys. Rev. D **95**, 085021 (2017).
[51] A. Betti, S. Bolognesi, S. B. Gudnason, K. Konishi, and K. Ohashi, J. High Energy Phys. 01 (2018) 106.
[52] A. Flachi, M. Nitta, S. Takada, and R. Yoshii, Phys. Lett. B **798**, 134999 (2019).
[53] S. Bolognesi, S. B. Gudnason, K. Konishi, and K. Ohashi, J. High Energy Phys. 06 (2018) 064.
[54] M. N. Chernodub, V. A. Goy, and A. V. Molochkov, Proc. Sci., Confinement2018 (**2019**) 006, [arXiv:1901.04754].
[55] D. Pavshinkin, arXiv:1905.02416.
[56] M. Fukugita, H. Mino, M. Okawa, and A. Ukawa, Phys. Rev. Lett. **65**, 816 (1990).
[57] G. V. Dunne and M. Ünsal, J. High Energy Phys. 11 (2012) 170.
[58] G. V. Dunne and M. Ünsal, Phys. Rev. D **87**, 025015 (2013).
[59] Y. Tanizaki, T. Misumi, and N. Sakai, J. High Energy Phys. 12 (2017) 056.
[60] M. Asakawa, T. Hatsuda, E. Itou, M. Kitazawa, and H. Suzuki (FlowQCD Collaboration), Phys. Rev. D **90**, 011501 (2014); **92**, 059902(E) (2015).
[61] H. Makino and H. Suzuki, Prog. Theor. Exp. Phys. **2015**, 033B08 (2015).
[62] H. Makino, F. Sugino, and H. Suzuki, Prog. Theor. Exp. Phys. **2015**, 043B07 (2015).
[63] M. Teper, Acta Phys. Pol. B **40**, 3249 (2009).
[64] M. Caselle, A. Nada, and M. Panero, J. High Energy Phys. 07 (2015) 143; 11 (2017) 016(E).
[65] M. Luscher and P. Weisz, J. High Energy Phys. 07 (2004) 014.
[66] T. Sulejmanpasic, Phys. Rev. Lett. **118**, 011601 (2017).
[67] M. Eto, Y. Isozumi, M. Nitta, K. Ohashi, and N. Sakai, Phys. Rev. D **72**, 025011 (2005).
[68] M. Eto, T. Fujimori, Y. Isozumi, M. Nitta, K. Ohashi, K. Ohta, and N. Sakai, Phys. Rev. D **73**, 085008 (2006).
[69] F. Bruckmann, Phys. Rev. Lett. **100**, 051602 (2008).
[70] W. Brendel, F. Bruckmann, L. Janssen, A. Wipf, and C. Wozar, Phys. Lett. B **676**, 116 (2009).
[71] E. Itou, J. High Energy Phys. 05 (2019) 093.
[72] M. Nitta, J. High Energy Phys. 03 (2015) 108.
[73] M. Nitta, J. High Energy Phys. 08 (2015) 063.
[74] Z. Wan and J. Wang, arXiv:1812.11968.
[75] T. Misumi, M. Nitta, and N. Sakai, J. High Energy Phys. 06 (2014) 164.
[76] T. Misumi, M. Nitta, and N. Sakai, J. High Energy Phys. 09 (2015) 157.
[77] P. V. Buividovich, G. V. Dunne, and S. N. Valgushev, Phys. Rev. Lett. **116**, 132001 (2016).
[78] T. Fujimori, S. Kamata, T. Misumi, M. Nitta, and N. Sakai, Phys. Rev. D **94**, 105002 (2016).
[79] T. Fujimori, S. Kamata, T. Misumi, M. Nitta, and N. Sakai, Phys. Rev. D **95**, 105001 (2017).
[80] T. Fujimori, S. Kamata, T. Misumi, M. Nitta, and N. Sakai, Prog. Theor. Exp. Phys. **2017**, 083B02 (2017).
[81] D. Dorigoni and P. Glass, SciPost Phys. **4**, 012 (2018).
[82] T. Fujimori, S. Kamata, T. Misumi, M. Nitta, and N. Sakai, J. High Energy Phys. 02 (2019) 190.